JOHANNES KEPLER UNIVERSITY LINZ

Institute of Computational Mathematics

Shape Optimization of an Electric Motor Subject to Nonlinear Magnetostatics

Peter Gangl
Doctoral Program "Computational Mathematics" (W1214)
Johannes Kepler University
Altenberger Str. 69, 4040 Linz, Austria

Ulrich Langer
Institute of Computational Mathematics, Johannes Kepler University
and
Johann Radon Institute for Computational and Applied Mathematics
Austrian Academy of Sciences
Altenberger Str. 69, 4040 Linz, Austria

Antoine Laurain
and
Houcine Meftahi
Institut für Mathematik, Technical University of Berlin
Str. des 17. Juni 136, 10623 Berlin

Kevin Sturm
Fakultät für Mathematik, Universität Duisburg-Essen
Thea-Leymann-Str. 9, 45127 Essen

NuMa-Report No. 2015-01 January 2015

Technical Reports before 1998:

1995

95-1	Hedwig Brandstetter *Was ist neu in Fortran 90?*	March 1995
95-2	G. Haase, B. Heise, M. Kuhn, U. Langer *Adaptive Domain Decomposition Methods for Finite and Boundary Element Equations.*	August 1995
95-3	Joachim Schöberl *An Automatic Mesh Generator Using Geometric Rules for Two and Three Space Dimensions.*	August 1995

1996

96-1	Ferdinand Kickinger *Automatic Mesh Generation for 3D Objects.*	February 1996
96-2	Mario Goppold, Gundolf Haase, Bodo Heise und Michael Kuhn *Preprocessing in BE/FE Domain Decomposition Methods.*	February 1996
96-3	Bodo Heise *A Mixed Variational Formulation for 3D Magnetostatics and its Finite Element Discretisation.*	February 1996
96-4	Bodo Heise und Michael Jung *Robust Parallel Newton-Multilevel Methods.*	February 1996
96-5	Ferdinand Kickinger *Algebraic Multigrid for Discrete Elliptic Second Order Problems.*	February 1996
96-6	Bodo Heise *A Mixed Variational Formulation for 3D Magnetostatics and its Finite Element Discretisation.*	May 1996
96-7	Michael Kuhn *Benchmarking for Boundary Element Methods.*	June 1996

1997

97-1	Bodo Heise, Michael Kuhn and Ulrich Langer *A Mixed Variational Formulation for 3D Magnetostatics in the Space $H(rot) \cap H(div)$*	February 1997
97-2	Joachim Schöberl *Robust Multigrid Preconditioning for Parameter Dependent Problems I: The Stokes-type Case.*	June 1997
97-3	Ferdinand Kickinger, Sergei V. Nepomnyaschikh, Ralf Pfau, Joachim Schöberl *Numerical Estimates of Inequalities in $H^{\frac{1}{2}}$.*	August 1997
97-4	Joachim Schöberl *Programmbeschreibung NAOMI 2D und Algebraic Multigrid.*	September 1997

From 1998 to 2008 technical reports were published by SFB013. Please see
`http://www.sfb013.uni-linz.ac.at/index.php?id=reports`
From 2004 on reports were also published by RICAM. Please see
`http://www.ricam.oeaw.ac.at/publications/list/`
For a complete list of NuMa reports see
`http://www.numa.uni-linz.ac.at/Publications/List/`

Shape optimization of an electric motor subject to nonlinear magnetostatics

P. Gangl [*1], U. Langer [†1,2], A. Laurain [‡3], H. Meftahi [§3], and K. Sturm [¶4]

[1]Johannes Kepler University, Altenberger Straße 69, A-4040 Linz, Austria
[2]RICAM, Altenberger Straße 69, A-4040 Linz, Austria
[3]Technical University of Berlin, Str. des 17. Juni 136, 10623 Berlin
[4]Universität Duisburg-Essen, Fakultät für Mathematik

Abstract

The goal of this paper is to improve the performance of an electric motor by modifying the geometry of a specific part of the iron core of its rotor. To be more precise, the objective is to smooth the rotation pattern of the rotor. A shape optimization problem is formulated by introducing a tracking-type cost functional to match a desired rotation pattern. The magnetic field generated by permanent magnets is modeled by a nonlinear partial differential equation of magnetostatics. The shape sensitivity analysis is rigorously performed for the nonlinear problem by means of a new shape-Lagrangian formulation adapted to nonlinear problems.

Keywords: electric motor, shape optimization, magnetostatics, nonlinear partial differential equations.

1 Introduction

Advanced shape optimization techniques have become a key tool for the design of industrial structures. In the automotive and aeronautic industries, for instance, the reduction of the drag or of the noise are important features which can be reduced by changing the design of the vehicles. In general, when considering a complex mechanical assemblage, it is often possible to optimize the geometry of certain pieces to improve the overall performance of the object. In the industrial sector, the shape optimization of electrical machines is the most economical approach to improve their efficiency and performance. Shape optimization problems are usually formulated as the minimization of a given cost function,

[*]peter.gangl@dk-compmath.jku.at
[†]ulrich.langer@ricam.oeaw.ac.at
[‡]laurain@math.tu-berlin.de
[§]meftahi@math.tu-berlin.de
[¶]kevin.sturm@uni-due.de

typical examples being the weight or the compliance for elastic systems. The most interesting and challenging problems of these type have linear or nonlinear partial differential equations constraints; see, for instance, [1, 7, 9, 14, 15, 18, 19, 22, 26, 27, 28, 29, 37, 38, 40] and the references therein.

In this work, a shape optimization approach is used to improve the design of an electric motor in order to match a desired smoother rotation pattern. As a model problem, we consider an interior permanent magnet (IPM) brushless electric motor consisting of a rotor (inner part) and a stator (outer part) separated by a thin air gap and containing both an iron core; see Fig. 1 for a description of the geometry. The rotor contains permanent magnets. The coil areas are located on the inner part of the stator. In general, inducing current in the coils initiates a movement of the rotor due to the interaction between the magnetic fields generated by the electric current and by the magnets. In our application, we are only interested in the magnetic field B for a fixed rotor position without any current induced. Since the magnetic properties of copper in the coils and of air are similar, we model these regions as air regions, too. We refer the reader to [6, 20, 31, 32] for other approaches to the design optimization of IPM electric motors and to [43] for a special method of modeling IPM motors using radial basis functions.

Due to practical restrictions, only some specific parts of the geometry can be modified. In our application, we identify a design subregion Ω of the iron core of the rotor subject to the shape optimization process. Our objective is to modify Ω in order to match a desired rotation pattern as well as possible. Practically this is achieved by tracking a certain desired profile of the magnetic flux density, which is done by reformulating the problem as a shape optimization one by introducing a tracking-type cost function.

The shape optimization of Ω has been considered in [11] from the point of view of the topological sensitivity [34, 39]. However, the derivation of the so-called *topological derivative* for nonlinear problems is formal since the mathematical theory for these problems is still in its early stages; see [4, 10, 21] for a few results in this direction. Moreover, the drawback of the topological derivative is that it usually creates geometries with jagged contours.

In this paper, we focus on the shape optimization of the design domain Ω by means of the *shape derivative*, which, contrarily to the topological derivative, proceeds by smooth deformation of the boundary of a reference design. In this way, the optimal shape has a smooth boundary provided that the numerical algorithm is carefully devised. Computing the shape derivative for problems depending on linear partial differential equations is a well-understood topic; see for instance [7, 17, 40]. For nonlinear problems, the literature is scarcer and the computation of the shape derivative is often formal. A novel aspect of this paper is to provide an efficient and rigorous way to compute the shape derivative of the cost functional without the need to compute the material derivative of the solution of the nonlinear state equation. The method is based on a novel Lagrangian method for nonlinear problems and on the volume expression of the shape derivative; see [29, 41]. This allows to obtain a smooth deformation field used as a descent direction in a gradient method. In the numerical algorithm, the mesh is deformed iteratively using this vector field until it reaches an equilibrium state.

The rest of the paper is organized as follows: In Section 2, we formulate the shape optimization problem and give the underlying nonlinear magnetostatic equation. Existence of a solution to the shape optimization problem is shown in Section 3. In Section 4, we introduce the general notion of a shape derivative and give an abstract differentiability re-

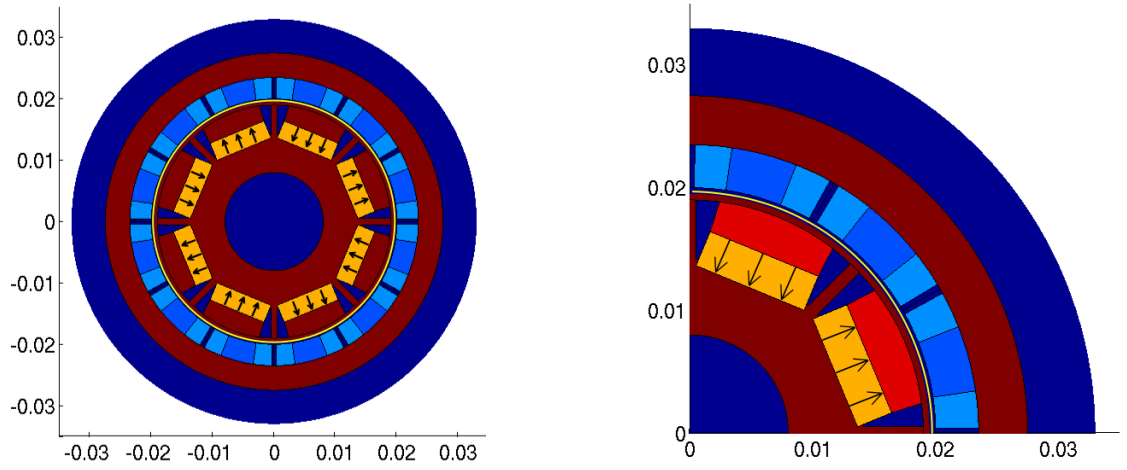

(a) (b)

Figure 1: (a) Geometry of the electric motor with permanent magnet areas Ω_{ma} (orange with arrows indicating the directions of magnetization), ferromagnetic material Ω_f^{ref} (brown), coil areas Ω_c (light blue), air Ω_a (dark blue) and thin air gap (yellow layer between rotor and stator); Γ_0 is a circle located in the air gap. (b) Zoom on the upper right quarter of the motor where the reference design area $\Omega^{\text{ref}} \subset \Omega_f^{\text{ref}}$ corresponds to the highlighted (red) region. The reference region Ω^{ref} is subject to the shape optimization procedure.

sult which is used later on to compute the shape derivative of the cost functional. Section 5 deals with the shape derivative of the cost functional. Finally, in Section 6, a numerical algorithm is presented to optimize the design of Ω, and numerical results showing the optimal shape are presented.

2 Problem formulation

Let $D \subset \mathbf{R}^2$ be the smooth bounded domain representing an IPM brushless electric motor as depicted in Fig. 1 with a ferromagnetic part $\Omega_f^{\text{ref}} \subset D$, permanent magnets $\Omega_{\text{ma}} \subset D$, air regions $\Omega_a \subset D$ and coil areas Ω_c. The design domain Ω is included in a reference domain $\Omega^{\text{ref}} \subset \Omega_f^{\text{ref}}$. The inner part of the motor is called the rotor and the outer part the stator. They are separated by a small air gap, the thin yellow circular layer in Fig. 1. By Γ_0 we denote a circle within the air gap. When an electric current is induced in the coils, the rotor containing the permanent magnets rotates. In reality the motor is a three-dimensional object, but considering the problem only on the cross-section of the motor is a modeling assumption that is commonly used; see [2, 3]. For a comparison between two- and three-dimensional models of electric motors, see [25, 42].

Denote $\Gamma := \partial\Omega$ the boundary of the optimized part Ω which is assumed to be Lipschitz. We introduce the variable ferromagnetic set $\Omega_f := (\Omega_f^{\text{ref}} \setminus \overline{\Omega^{\text{ref}}}) \cup \Omega$ and $\Gamma_f := \partial\Omega_f$. The permanent magnets create a magnetic field in D. In our application, we assume the coils to be switched off. Thus, no electric current is induced and the rotor is not moving. The magnetic field generated by the permanent magnets can be calculated via a boundary

value problem of the form

$$\begin{aligned} -\operatorname{div}(\beta_\Omega(x,|\nabla u|^2)\nabla u) &= f \quad \text{in } \Omega_f \text{ and } D\setminus\overline{\Omega}_f,\\ u &= 0 \quad \text{on } \partial D, \end{aligned} \tag{1}$$

with the transmission conditions on the interface Γ_f

$$\begin{aligned} [\![u]\!] &= 0 \quad \text{on} \quad \Gamma_f,\\ [\![\beta_\Omega(x,|\nabla u|^2)\partial_n u]\!] &= 0 \quad \text{on} \quad \Gamma_f, \end{aligned} \tag{2}$$

where n denotes the outward unit normal vector to Ω_f. Defining v^- the restriction of some function v on Ω_f and v^+ its restriction on $D\setminus\overline{\Omega_f}$ we denote by $[\![v]\!]$ the jump of v across the interface Γ_f, i.e.

$$[\![v]\!] = v^+|_{\Gamma_f} - v^-|_{\Gamma_f}.$$

The nonlinear, piecewise smooth function β is defined for $(x,\zeta)\in D\times\mathbf{R}$ as

$$\begin{aligned} \beta_\Omega(x,\zeta) &:= \beta_1(\zeta)\chi_{\Omega_f}(x) + \beta_2(\zeta)\chi_{D\setminus\overline{\Omega_f}}(x)\\ &= \beta_1(\zeta)(\chi_\Omega(x) + \chi_{\Omega_f^{\mathrm{ref}}\setminus\overline{\Omega^{\mathrm{ref}}}}(x)) + \beta_2(\zeta)(\chi_{D\setminus\overline{\Omega_f^{\mathrm{ref}}}}(x) + \chi_{\Omega^{\mathrm{ref}}\setminus\overline{\Omega}}(x)), \end{aligned}$$

where χ is the indicator function of a given set. Note that the expression above is meaningful since $\Omega\subset\Omega^{\mathrm{ref}}\subset\Omega_f^{\mathrm{ref}}$. The weak form of (1) reads

$$\text{Find } u\in H_0^1(D) \text{ such that } \int_D \beta_\Omega(x,|\nabla u|^2)\nabla u\cdot\nabla v\,\mathrm{d}x = \langle f,v\rangle \quad \forall v\in H_0^1(D), \tag{3}$$

where $\langle\cdot,\cdot\rangle$ denotes the duality bracket between $H^{-1}(D)$ and $H_0^1(D)$. The scalar function u is the third component of the vector potential of the magnetic flux density in three dimensions, $B = \operatorname{curl}((0,0,u)^T)$. In our model, we consider the restriction of B to a two-dimensional cross-section since the third component vanishes.

In the sequel, we make the following assumption for β_1 and β_2:

Assumption 1. *The functions $\beta_1,\beta_2:\mathbf{R}\to\mathbf{R}$ satisfy the following conditions:*

1. *There exist constants $c_1,c_2,c_3,c_4>0$, such that*

$$c_1\le\beta_1(\zeta)\le c_2, \quad c_3\le\beta_2(\zeta)\le c_4 \quad \text{for all } \zeta\in\mathbf{R}.$$

2. *The function $s\mapsto\beta_i(s^2)s$ is strongly monotone with monotonicity constant m and Lipschitz continuous with Lipschitz constant L:*

$$\begin{aligned} (\beta_i(s^2)\,s-\beta_i(t^2)\,t)\,(s-t) &\ge m(s-t)^2 && \text{for all } s,t\ge 0,\\ |\beta_i(s^2)\,s-\beta_i(t^2)\,t| &\le L|s-t| && \text{for all } s,t\ge 0. \end{aligned}$$

3. *The functions β_1,β_2 are in $C^1(\mathbf{R})$.*

4. *There exist constants $\lambda,\Lambda>0$ such that for $i=1,2$,*

$$\lambda|\eta|^2\le\beta_i(|\rho|^2)|\eta|^2+2\beta_i'(|\rho|^2)(\eta\cdot\rho)^2\le\Lambda|\eta|^2 \quad \text{for all } \eta,\rho\in\mathbf{R}^2.$$

The task is to modify the shape of the design region $\Omega \subset \Omega^{\text{ref}}$ in such a way that the radial component of the resulting magnetic flux density on the circle Γ_0 in the air gap fits a given data as good as possible. We consider the following minimization problem:

$$\begin{cases} \text{minimize } J(\Omega, u) := \displaystyle\int_{\Gamma_0} |B_r(u) - B_d|^2 \mathrm{d}s \\ \text{subject to } \Omega \in \mathcal{O} \text{ and } u \text{ solution of (3)} \end{cases} \tag{4}$$

where

$$\mathcal{O} = \left\{ \Omega \subset \Omega^{\text{ref}} \subset \Omega_f^{\text{ref}}, \Omega \text{ open and Lipschitz with uniform Lipschitz constant } L_{\mathcal{O}} \right\} \tag{5}$$

and $\Gamma_0 \subset D$ is a smooth one-dimensional subset of D. The sets Ω^{ref} and Ω_f^{ref} are reference domains; see Fig. 1. Here, $B_r(u) = \nabla u \cdot \tau$ where τ is the tangential vector to Γ_0 and $B_d \in C^1(\Gamma_0)$ denotes the given desired radial component of the magnetic flux density along the air gap. In order to obtain the first-order optimality conditions for this minimization problem we compute the derivative of J with respect to the shape Ω.

Remark 1. *Let us note that*

- *in our application, the right-hand side f represents the magnetization of the permanent magnets. In general, it can be a combination of magnetization and impressed currents in the coils.*
- *the link between β and the magnetic reluctivity is $\beta(s) = \nu(\sqrt{s})$. In this case, the boundary value problem (1) is called the two-dimensional magnetostatic boundary value problem; see [23, 36]. We will see in Section 6 that Assumption 1 is satisfied for ν due to physical properties.*
- *the Dirichlet condition $u|_{\partial D} = 0$ implies $B \cdot n = 0$, thus no magnetic flux can leave the computational domain D.*

Given Assumption 1, we can state existence and uniqueness of a solution u to the state equation (3).

Theorem 1. *Assume that Assumption 1.1 and 1.2 hold. Then problem (3) admits a unique solution $u \in H_0^1(D)$ for any fixed right-hand side $f \in H^{-1}(D)$ and we have the estimate*

$$\|u\|_{H_0^1(D)} \leq c \|f\|_{H^{-1}(D)}.$$

Proof. A proof can be found in [16, 35, 44]. □

3 Existence of optimal shapes

In this section, we prove that problem (4) has a solution $\Omega^\star$. We make use of the following result [17, Theorem 2.4.10]

Theorem 2. *Let Ω_n be a sequence in $\mathcal{O}$. Then there exists $\Omega \in \mathcal{O}$ and a subsequence Ω_{n_k} which converges to Ω in the sense of Hausdorff, and in the sense of characteristic functions. In addition, $\overline{\Omega}_{n_k}$ and $\partial\Omega_{n_k}$ converge in the sense of Hausdorff respectively towards $\overline{\Omega}$ and $\partial\Omega$.*

Let $\Omega_n \in \mathcal{O}$ be a minimizing sequence for problem (4). According to Theorem 2, we can extract a subsequence, which we still denote Ω_n, which converges to some $\Omega \in \mathcal{O}$. Denote u_n and u the solutions of (1)-(2) with Ω_n and Ω, respectively. We prove that $u_n \to u$ in $H_0^1(D)$.

First of all in view of Theorem 1 we have

$$\|u_n\|_{H_0^1(D)} \leq c\|f\|_{H^{-1}(D)} \tag{6}$$

where c depends only on D. Thus we may extract a subsequence u_n such that $u_n \to u^\star$ in $L^2(D)$ and $\nabla u_n \rightharpoonup \nabla u^\star$ weakly in $L^2(\Omega)$. Extracting yet another subsequence, we may as well assume that $\Omega_n \to \Omega^\star$ in the sense of characteristic functions applying Theorem 2.

Subtracting the variational formulation for two elements u_n and u_m of the sequence and choosing the test function $v = u_n - u_m$ we get

$$\int_D \big((\beta_{\Omega_n}(x, |\nabla u_n|^2)\nabla u_n - (\beta_{\Omega_m}(x, |\nabla u_m|^2)\nabla u_m\big) \cdot \nabla(u_n - u_m)\,\mathrm{d}x = 0 \tag{7}$$

Let us introduce for simplicity the notation $\beta_1^n := \beta_1(|\nabla u_n|^2)$ and $\beta_2^n := \beta_2(|\nabla u_n|^2)$. Then (7) becomes

$$\begin{aligned}&\int_D (\beta_1^n(\chi_{\Omega_n} + \chi_{\Omega_f^{\mathrm{ref}}\setminus\Omega^{\mathrm{ref}}}) + \beta_2^n(\chi_{D\setminus\Omega_f^{\mathrm{ref}}} + \chi_{\Omega^{\mathrm{ref}}\setminus\Omega_n}))\nabla u_n \cdot \nabla(u_n - u_m)\\ &- (\beta_1^m(\chi_{\Omega_m} + \chi_{\Omega_f^{\mathrm{ref}}\setminus\Omega^{\mathrm{ref}}}) + \beta_2^m(\chi_{D\setminus\Omega_f^{\mathrm{ref}}} + \chi_{\Omega^{\mathrm{ref}}\setminus\Omega_m}))\nabla u_m \cdot \nabla(u_n - u_m)\,\mathrm{d}x = 0\end{aligned}$$

This yields

$$I_1 + I_2 + I_3 + I_4 + I_5 + I_6 = 0 \tag{8}$$

where

$$\begin{aligned}I_1 &:= \int_D (\chi_{\Omega_n} - \chi_{\Omega_m})\beta_1^n \nabla u_n \cdot \nabla(u_n - u_m)\,dx,\\ I_2 &:= \int_D \chi_{\Omega_m}(\beta_1^n \nabla u_n - \beta_1^m \nabla u_m) \cdot \nabla(u_n - u_m)\,dx,\\ I_3 &:= \int_D \chi_{\Omega_f^{\mathrm{ref}}\setminus\Omega^{\mathrm{ref}}}(\beta_1^n \nabla u_n - \beta_1^m \nabla u_m) \cdot \nabla(u_n - u_m)\,dx,\\ I_4 &:= \int_D \chi_{D\setminus\Omega_f^{\mathrm{ref}}}(\beta_2^n \nabla u_n - \beta_2^m \nabla u_m) \cdot \nabla(u_n - u_m)\,dx,\\ I_5 &:= \int_D (\chi_{\Omega^{\mathrm{ref}}\setminus\Omega_n} - \chi_{\Omega^{\mathrm{ref}}\setminus\Omega_m})\beta_2^n \nabla u_n \cdot \nabla(u_n - u_m)\,dx,\\ I_6 &:= \int_D \chi_{\Omega^{\mathrm{ref}}\setminus\Omega_m}(\beta_2^n \nabla u_n - \beta_2^m \nabla u_m) \cdot \nabla(u_n - u_m)\,dx.\end{aligned}$$

To estimate the above integrals, we use the following lemma:

Lemma 1. *Let $p, q \in \mathbf{R}^2$. If Assumption 1.2 holds, then*

$$[\beta_i(|p|^2)p - \beta_i(|q|^2)q] \cdot (p - q) \geq m|p - q|^2.$$

Proof. Using Assumption 1.2 we compute

$$\begin{aligned}
&[\beta_i(|p|^2)p - \beta_i(|q|^2)q]\cdot(p-q)\\
&\quad= m|p-q|^2 + [(\beta_i(|p|^2)-m)p - (\beta_i(|q|^2)-m)q]\cdot(p-q)\\
&\quad= m|p-q|^2 + \underbrace{(\beta_i(|p|^2)-m)}_{\geq 0}\underbrace{(|p|^2 - p\cdot q)}_{\geq |p|(|p|-|q|)} - \underbrace{(\beta_i(|q|^2)-m)}_{\geq 0}\underbrace{(p\cdot q - |q|^2)}_{\leq |q|(|p|-|q|)}\\
&\quad= m|p-q|^2 + \underbrace{(\beta_i(|p|^2)|p| - \beta_i(|q|^2)|q|)(|p|-|q|)}_{\geq m(|p|-|q|)^2} - m(|p|-|q|)^2\\
&\quad\geq m|p-q|^2.
\end{aligned}$$

□

Applying Lemma 1 with $p = \nabla u_n$ and $q = \nabla u_m$ we get

$$\begin{aligned}
I_2 + I_3 + I_4 + I_6 &\geq m\int_D (\chi_{\Omega_m} + \chi_{\Omega_f^{\mathrm{ref}}\setminus\Omega^{\mathrm{ref}}} + \chi_{D\setminus\Omega_f^{\mathrm{ref}}} + \chi_{\Omega^{\mathrm{ref}}\setminus\Omega_m})|\nabla u_n - \nabla u_m|^2\,dx\\
&= m\int_D |\nabla u_n - \nabla u_m|^2\,dx. \qquad (9)
\end{aligned}$$

Hölder's inequality yields

$$|I_1| \leq \|\beta_1^n\|_{L^\infty(D)}\|\chi_{\Omega_n} - \chi_{\Omega_m}\|_{L^r(D)}\|\nabla u_n\|_{L^2(D)}\|\nabla(u_n - u_m)\|_{L^s(D)}$$

with $r^{-1} + s^{-1} = 1/2$, $r, s \geq 1$. Performing a similar estimate for I_5 and in view of Assumption 1.1 this yields

$$|I_1| \leq c_2\|\chi_{\Omega_n} - \chi_{\Omega_m}\|_{L^r(D)}\|\nabla u_n\|_{L^2(D)}\|\nabla(u_n - u_m)\|_{L^s(D)} \qquad (10)$$
$$|I_5| \leq c_4\|\chi_{\Omega_n} - \chi_{\Omega_m}\|_{L^r(D)}\|\nabla u_n\|_{L^2(D)}\|\nabla(u_n - u_m)\|_{L^s(D)} \qquad (11)$$

Using equality (8) and inequalities (6),(9),(10),(11) we obtain the estimate

$$\int_D |\nabla u_n - \nabla u_m|^2\,dx \leq c\|\chi_{\Omega_n} - \chi_{\Omega_m}\|_{L^r(D)}\|f\|_{H^{-1}(D)}\|\nabla(u_n - u_m)\|_{L^s(D)}$$

Since χ_{Ω_n} is a characteristic function, the parameter r can be chosen arbitrarily large, and consequently, s can be chosen arbitrarily close to 2. Therefore, assuming a little more regularity than H^1 for the solution of (3), the convergence of the characteristic functions of Ω_n in $L^p(D)$ implies the strong convergence of u_n towards $u^\star$ in $H_0^1(D)$. Consequently, we obtain the following result:

Proposition 1. *Let $\Omega_n \in \mathcal{O}$ be a minimizing sequence for problem (4) and Ω be an accumulation point of this sequence as in Theorem 2. Assume there exists $\varepsilon > 0$ such that the solution u of (3) satisfies*

$$\|u\|_{H^{1+\varepsilon}(D)\cap H_0^1(D)} \leq c$$

where c depends only on f and D. Then the sequence $u_n \in H_0^1(D)$ corresponding to Ω_n converges to u strongly in $H_0^1(D)$, where u is the solution of (3) in Ω.

Proof. We have seen that there exists $u^\star \in H_0^1(D)$ such that $u_n \to u^\star$ in $H_0^1(D)$. We just need to prove that $u^\star = u$. The strong convergence of u_n in $H_0^1(D)$ yields $\nabla u_n \to \nabla u^\star$ pointwise almost everywhere in D, and also the pointwise almost everywhere (a.e.) convergence $\beta_i^n \to \beta_i(|\nabla u^\star|^2)$ for $i = 1, 2$. We also have the pointwise a.e. convergence of the characteristic function χ_{Ω_n} to $\chi_{\Omega^\star}$ which implies the pointwise a.e. convergence $\beta_{\Omega_n}(\cdot, |\nabla u_n|^2) \to \beta_{\Omega^\star}(\cdot, |\nabla u^\star|^2)$. Next, the weak formulation for u_n is

$$\int_D \beta_{\Omega_n}(x, |\nabla u_n|^2)\nabla u_n \cdot \nabla v \, \mathrm{d}x = \langle f, v\rangle \quad \text{for all } v \in H_0^1(D),$$

The strong convergence of u_n in $H_0^1(D)$ and the pointwise convergence of $\beta_{\Omega_n}(\cdot, |\nabla u_n|^2)$ implies

$$\int_D \beta_{\Omega^\star}(x, |\nabla u^\star|^2)\nabla u^\star \cdot \nabla v \, \mathrm{d}x = \langle f, v\rangle \quad \text{for all } v \in H_0^1(D),$$

which proves finally $u^\star = u$. □

Remark 2. *In fact we have proven a stronger result, i.e., the Lipschitz continuity of u_n in $H_0^1(D)$ with respect to the characteristic function χ_{Ω_n}.*

4 Shape derivative

4.1 Preliminaries

In this section, we recall some basic facts about the velocity method in shape optimization used to transform a reference shape; see [7, 40]. In the velocity method, also known as speed method, a domain $\Omega \subset D \subset \mathbf{R}^2$ is deformed by the action of a velocity field V defined on D. Suppose that D is a Lipschitz domain and denote its boundary $\Sigma := \partial D$. The domain evolution is described by the solution of the dynamical system

$$\frac{d}{dt}x(t) = V(x(t)), t \in [0, \varepsilon), \quad x(0) = X \in \mathbf{R}^2 \tag{12}$$

for some real number $\varepsilon > 0$. Suppose that V is continuously differentiable and has compact support in D, i.e. $V \in \mathcal{D}^1(D, \mathbf{R}^2)$. Then the ordinary differential equation (12) has a unique solution on $[0, \varepsilon)$. This enables us to define the diffeomorphism

$$T_t : \mathbf{R}^2 \to \mathbf{R}^2; X \mapsto T_t(X) := x(t). \tag{13}$$

With this choice of V, the domain D is globally invariant by the transformation T_t, i.e. $T_t(D) = D$ and $T_t(\partial D) = \partial D$. For $t \in [0, \varepsilon)$, T_t is invertible. Furthermore, for sufficiently small $\tau > 0$, the Jacobian determinant

$$\xi(t) := \det DT_t \tag{14}$$

of T_t is strictly positive. In the sequel, we use the notation DT_t^{-1} for the inverse of DT_t and DT_t^{-T} for the transpose of the inverse. We also denote by

$$\xi_\tau(t) := \xi(t)|DT_t^{-T}n| \tag{15}$$

the tangential Jacobian of T_t on ∂D.
Then the following lemma holds [7]:

Lemma 2. *For $\varphi \in W^{1,1}_{loc}(\mathbf{R}^2)$ and $V \in \mathcal{D}^1(\mathbf{R}^2, \mathbf{R}^2)$ we have*

$$\nabla(\varphi \circ T_t) = DT_t^T(\nabla\varphi) \circ T_t, \qquad \frac{d}{dt}(\varphi \circ T_t) = (\nabla\varphi \cdot V) \circ T_t,$$
$$\frac{d\xi(t)}{dt} = \xi(t)\,[\operatorname{div} V(t)] \circ T_t, \qquad \xi_\tau'(0) = \operatorname{div}_{\partial D} V := \operatorname{div} V|_{\partial D} - DVn \cdot n.$$

Definition 1. *Suppose we are given a real valued shape function J defined on a subset Ξ of the powerset $2^{\mathbf{R}^2}$. We say that J is Eulerian semi-differentiable at $\Omega \in \Xi$ in the direction V if the following limit exists in $\mathbf{R}$*

$$dJ(\Omega; V) := \lim_{t \searrow 0} \frac{J(T_t(\Omega)) - J(\Omega)}{t}.$$

If the map $V \longrightarrow dJ(\Omega; V)$ is linear and continuous with respect to the topology of $\mathcal{D}(D, \mathbf{R}^2) := C_c^\infty(D, \mathbf{R}^2)$, then J is said to be shape differentiable at Ω and $dJ(\Omega; V)$ is called the shape derivative of J.

4.2 An abstract differentiability result

Let E and F be Banach spaces. Let G be a function

$$G : [0, \tau] \times E \times F \to \mathbf{R}, \quad (t, \varphi, \psi) \mapsto G(t, \varphi, \psi) \tag{16}$$

and define

$$E(t) := \{u \in E |\ d_\psi G(t, u, 0; \hat{\psi}) = 0 \ \text{ for all } \hat{\psi} \in F\}. \tag{17}$$

Let us introduce the following hypotheses.

Assumption 2 (H0)**.** *For every $(t, \psi) \in [0, \tau] \times F$, we assume that*

(i) the set $E(t)$ is single-valued and we write $E(t) = \{u^t\}$,

(ii) the function $[0, 1] \ni s \mapsto G(t, su^t + s(u^t - u^0), \psi)$ is absolutely continuous,

(iii) the function $[0, 1] \ni s \mapsto d_\varphi G(t, su^t + (1 - s)u^0, \psi; \varphi)$ belongs to $L^1(0, 1)$ for all $\varphi \in E$,

(iv) the function $\tilde{\psi} \mapsto G(t, u, \tilde{\psi})$ is affine-linear.

For $t \in [0, \tau]$ and $u^t \in E(t)$, let us introduce the set

$$Y(t, u^t, u^0) := \left\{ q \in F |\ \forall \hat{\varphi} \in E : \int_0^1 d_\varphi G(t, su^t + (1 - s)u^0, q; \hat{\varphi})\, ds = 0 \right\}, \tag{18}$$

which is called solution set of the *averaged adjoint equation* with respect to t, u^t and u^0. Note that $Y(0, u^0, u^0)$ coincides with the solution set of the usual adjoint state equation:

$$Y(0, u^0, u^0) = \left\{ q \in F |\ d_\varphi G(0, u^0, q; \hat{\varphi}) = 0 \quad \text{for all } \hat{\varphi} \in E \right\}. \tag{19}$$

The following result, proved in [41] allows us to compute the Eulerian semi-derivative of Definition 1 without computing the material derivative $\dot{u}$. The key is the introduction of the set (18).

Theorem 3. *Let Assumption (H0) hold and the following conditions be satisfied.*

(H1) For all $t \in [0,\tau]$ and all $\psi \in F$ the derivative $\partial_t G(t,u^0,\psi)$ exists.

(H2) For all $t \in [0,\tau]$, the set $Y(t,u^t,u^0)$ is single-valued and we write $Y(t,u^t,u^0) = \{p^t\}$.

(H3) For any sequence of non-negative real numbers $(t_n)_{n\in\mathbf{N}}$ converging to zero, there exists a subsequence $(t_{n_k})_{k\in\mathbf{N}}$ such that

$$\lim_{\substack{k\to\infty \\ s\searrow 0}} \partial_t G(s,u^0,p^{t_{n_k}}) = \partial_t G(0,u^0,p^0).$$

Then for $\psi \in F$ we obtain

$$\frac{d}{dt}(G(t,u^t,\psi))|_{t=0} = \partial_t G(0,u^0,p^0). \tag{20}$$

4.3 Adjoint equation

Introduce the Lagrangian associated to the minimization problem (4) for all $\varphi,\psi \in H_0^1(D)$:

$$G(\Omega,\varphi,\psi) := \int_{\Gamma_0} |B_r(\varphi) - B_d|^2\, ds + \int_D \beta(x,|\nabla u|^2)\nabla\varphi\cdot\nabla\psi\, dx - \langle f,\psi\rangle \tag{21}$$

The adjoint state equation is obtained by differentiating G with respect to φ at $\varphi = u$ and $\psi = p$,

$$d_\varphi G(\Omega,u,p;\varphi) = 0 \quad \text{for all } \varphi \in H_0^1(D),$$

or, equivalently,

$$\begin{aligned} &2\int_D \partial_\zeta\beta(x,|\nabla u|^2)(\nabla u\cdot\nabla\varphi)(\nabla u\cdot\nabla p)\, dx + \int_D \beta(x,|\nabla u|^2)\nabla p\cdot\nabla\varphi\, dx \\ &= -2\int_{\Gamma_0}(B_r(u)-B_d)B_r(\varphi)\, ds \quad \text{for all } \varphi \in H_0^1(D). \end{aligned} \tag{22}$$

Introduce the mean curvature κ of Γ_0 and the Laplace-Beltrami operator Δ_τ on Γ_0:

$$\Delta_\tau u := \Delta u - \kappa\frac{\partial u}{\partial n} - \frac{\partial^2 u}{\partial n^2}$$

Using $B_r(u) = \nabla_\tau u$ as well as the equalities

$$\begin{aligned} (\nabla u\cdot\nabla\varphi)(\nabla u\cdot\nabla p) &= ((\nabla u\otimes\nabla u)\nabla p)\cdot\nabla\varphi, \\ \int_{\Gamma_0}(\nabla_\tau u - B_d)\cdot\nabla_\tau\varphi\, ds &= -\int_{\Gamma_0}\Delta_\tau u\varphi - \varphi\kappa B_d\cdot n\, ds \end{aligned}$$

and Green's formula, we deduce the corresponding strong form of (22)

$$\begin{aligned} -\operatorname{div}(\mathcal{A}_1(\nabla u)\nabla p) &= 0 \quad \text{in } \Omega, \\ -\operatorname{div}(\mathcal{A}_2(\nabla u)\nabla p) &= 0 \quad \text{in } D\setminus\overline{\Omega}, \\ p &= 0 \quad \text{on } \partial D, \end{aligned} \tag{23}$$

with the transmission conditions

$$\begin{aligned} [p]_\Gamma &= 0 \quad \text{on } \Gamma, \\ [\mathcal{A}(\nabla u)\nabla p \cdot n]_\Gamma &= 0 \quad \text{on } \Gamma, \\ [\mathcal{A}(\nabla u)\nabla p \cdot n]_{\Gamma_0} &= 2\left(\Delta_\tau u - \kappa B_d \cdot n\right) \text{ on } \Gamma_0, \end{aligned} \tag{24}$$

where

$$\begin{aligned} \mathcal{A}(\nabla u) &:= \mathcal{A}_1(\nabla u)\chi_\Omega + \mathcal{A}_2(\nabla u)\chi_{D\setminus\Omega}, \\ \mathcal{A}_i(\nabla u) &:= \beta_i(|\nabla u|^2)I_2 + 2\partial_\zeta\beta_i(|\nabla u|^2)\nabla u \otimes \nabla u \in \mathbf{R}^{2,2}, \quad i = 1, 2. \end{aligned}$$

Note that, with this notation, the variational form of the equation can be written as

$$\int_D \mathcal{A}(\nabla u)\nabla p \cdot \nabla\varphi \, dx = -2\int_{\Gamma_0} (B_r(u) - B_d)B_r(\varphi)\, ds \quad \text{for all } \varphi \in H_0^1(D). \tag{25}$$

Now let us investigate the existence of a solution for the adjoint equation

Theorem 4. *Let Assumption 1.4 hold. For given $u \in H_0^1(D)$ the equation*

$$\int_D \mathcal{A}(\nabla u)\nabla p \cdot \nabla\varphi \, dx = -2\int_{\Gamma_0} (B_r(u) - B_d)B_r(\varphi)\, ds \quad \textit{for all } \varphi \in H_0^1(D). \tag{26}$$

has a unique solution $p \in H_0^1(D)$.

Proof. For fixed $u \in H_0^1(D)$, define the bilinear form

$$\begin{aligned} a'(u;\cdot,\cdot) : H_0^1(D) \times H_0^1(D) &\to \mathbb{R} \\ (v, w) &\mapsto \int_D \mathcal{A}(\nabla u)\nabla v \cdot \nabla w \, dx. \end{aligned}$$

We check the conditions of Lax-Milgram's theorem. The ellipticity of the bilinear form $a'(u;\cdot,\cdot)$ can be seen as follows:

$$a'(u; v, v) = \int_D \mathcal{A}(\nabla u)\nabla v \cdot \nabla v \, dx \geq \lambda \int_D |\nabla v|^2 \mathrm{d}x \geq \lambda\, C\|v\|^2_{H^1(D)}$$

where we have used the first estimate in Assumption 1.4. and Poincaré's inequality since $v \in H_0^1(D)$. The boundedness of the bilinear form $a'(u;\cdot,\cdot)$ can be seen by Hölder's inequality and again Assumption 1.4. The right-hand side is obviously a linear and continuous functional on $H_0^1(D)$,

$$\langle F_u, \varphi\rangle = -2\int_{\Gamma_0} (B_r(u) - B_d)B_r(\varphi)\, ds,$$

thus the theorem of Lax-Milgram yields the existence of a unique solution p to the variational problem

$$a'(u; \varphi, p) = \langle F_u, \varphi\rangle \quad \text{for all } \varphi \in H_0^1(D).$$

□

5 Shape derivative of the cost function

In this section we prove that the cost function J given by (4) is shape differentiable in the sense of Definition 1. Moreover, we derive a domain expression of the shape derivative. To be more precise, Theorem 3 is applied to show Theorem 5. Anticipating on the application of Section 6, we assume in what follows that f has the form

$$f = f_0 + \operatorname{div} M \text{ with } M = M_1 \chi_{\Omega_{\rm ma}}(x) + M_2 \chi_{D\setminus\Omega_{\rm ma}}(x)$$

where $f_0 \in H^1(D)$.

In this section we assume $\Omega \subset \Omega^{\rm ref}$, $V \in \mathcal{D}^1(\mathbf{R}^2, \mathbf{R}^2)$ and $\operatorname{supp}(V) \cap \Gamma_0 = \emptyset$. Denote $\Omega_k^{\rm ref}$, $k = 1, .., 8$, the connected components of $\Omega^{\rm ref}$ (see Fig. 1). Introduce $\Gamma^{\rm ref}$ the boundary of $\Omega^{\rm ref}$. The four sides of $\Gamma^{\rm ref}$ are denoted $\Gamma_k^{{\rm ref},N}, \Gamma_k^{{\rm ref},W}, \Gamma_k^{{\rm ref},E}, \Gamma_k^{{\rm ref},S}$ where the exponents mean "north", "south", "east", "west", respectively. We assume $V \cdot n = 0$ on $\Gamma_k^{{\rm ref},S}$ and $V \cdot n \leq 0$ on $\Gamma_k^{{\rm ref},E} \cup \Gamma_k^{{\rm ref},W} \cup \Gamma_k^{{\rm ref},N}$. These conditions guarantee that $\Omega_t := T_t(\Omega) \subset \Omega^{\rm ref}$. In addition, we assume that the vector field V is such that the transformation T_t satisfies $T_t(\Omega_{\rm ma}) = \Omega_{\rm ma}$ for t small enough.

Theorem 5. *Let β_1 and β_2 satisfy Assumption 1. Then the functional J is shape differentiable and its shape derivative in the direction V is given by*

$$\begin{aligned} dJ(\Omega; V) = &- \int_D (f_0 \operatorname{div}(V) + \nabla f_0 \cdot V) p \, dx \\ &+ \int_{\Omega_{ma}} \mathbb{P}'(0) \nabla p \cdot M_1 \, dx + \int_{D\setminus\overline{\Omega_{ma}}} \mathbb{P}'(0) \nabla p \cdot M_2 \, dx \\ &+ \int_D \beta_\Omega(x, |\nabla u|^2) \mathbb{Q}'(0) \nabla u \cdot \nabla p \, dx \\ &- \int_D 2 \partial_\zeta \beta_\Omega(x, |\nabla u|^2) (DV^T \nabla u \cdot \nabla u)(\nabla u \cdot \nabla p) \, dx \end{aligned} \tag{27}$$

where $\mathbb{P}'(0) = (\operatorname{div} V) I_2 - DV^T$, $\mathbb{Q}'(0) = (\operatorname{div} V) I_2 - DV^T - DV$, $I_2 \in \mathbb{R}^{2,2}$ is the identity matrix, and $u, p \in H_0^1(D)$ are respectively the solutions of the problems (1)-(2) *and* (23)-(24).

Remark 3. *Note that the last integral in* (27) *is well-defined thanks to Assumption 1.4. To see this, note that $V \in C^1(\overline{D}, \mathbf{R}^2)$, and that, for all $\zeta \in \mathbf{R}^2$, we have $\beta'(|\zeta|^2)|\zeta|^2 \leq \Lambda$. Hence*

$$\begin{aligned} \left| \int_D 2 \partial_\zeta \beta_\Omega(x, |\nabla u|^2) (DV^T \nabla u \cdot \nabla u)(\nabla u \cdot \nabla p) \, dx \right| &\leq C \int_D \partial_\zeta \beta_\Omega(x, |\nabla u|^2) |\nabla u|^2 |\nabla u \cdot \nabla p| \, dx \\ &\leq C\Lambda \int_D |\nabla u \cdot \nabla p| \, dx < \infty. \end{aligned} \tag{28}$$

The other terms in (27) *are obviously well-defined.*

Proof of Theorem 5. Let us consider the transformation T_t defined by (13) with $V \in \mathcal{D}^1(D, \mathbf{R}^2)$. In this case, $T_t(D) = D$, but, in general, $T_t(\Omega) := \Omega_t \neq \Omega$. We define the Lagrangian $G(\Omega_t, \varphi, \psi)$ at the transformed domain Ω_t for all φ, ψ in $H_0^1(D)$:

$$G(\Omega_t, \varphi, \psi) = \int_{\Gamma_0} |B_r(\varphi) - B_d|^2 \, ds + \int_D \beta_{\Omega_t}(x, |\nabla \varphi|^2) \nabla \varphi \cdot \nabla \psi \, dx - \langle f, \psi \rangle.$$

Since

$$f = f_0 + \operatorname{div} M \text{ with } M = M_1 \chi_{\Omega_{\mathrm{ma}}}(x) + M_2 \chi_{D\setminus\overline{\Omega_{\mathrm{ma}}}}(x)$$

where M_1 and M_2 are constant vectors, we transform the last term in G to

$$\langle f, \psi\rangle = \int_D f_0\psi + \langle \operatorname{div} M, \psi\rangle = \int_D f_0\psi - \int_D M\cdot\nabla\psi,$$

which yields

$$\begin{aligned} G(\Omega_t,\varphi,\psi) = &\int_{\Gamma_0} |B_r(\varphi) - B_d|^2 \, ds + \int_D \beta_{\Omega_t}(x, |\nabla\varphi|^2)\nabla\varphi\cdot\nabla\psi \, dx \\ &- \int_D f_0\psi + \int_{\Omega_{\mathrm{ma}}} M_1\cdot\nabla\psi + \int_{D\setminus\overline{\Omega_{\mathrm{ma}}}} M_2\cdot\nabla\psi. \end{aligned}$$

In order to differentiate $G(\Omega_t,\varphi,\psi)$ with respect to t, the integrals in $G(\Omega_t,\varphi,\psi)$ need to be transported back on the reference domain Ω using the transformation T_t. However, composing by T_t inside the integrals creates terms $\varphi\circ T_t$ and $\psi\circ T_t$ which might be non-differentiable. To avoid this problem, we need to parameterize the space $H_0^1(D)$ by composing the elements of $H_0^1(D)$ with T_t^{-1}. Following this argument, we introduce

$$\mathfrak{G}(t,\varphi,\psi) := G(\Omega_t, \varphi\circ T_t^{-1}, \psi\circ T_t^{-1}). \tag{29}$$

In (29), we proceed to the change of variable $x = T_t(\bar{x})$. This yields

$$\begin{aligned} \mathfrak{G}(t,\varphi,\psi) = &\int_{\Gamma_0} \xi_\tau(t)|B_r(\varphi) - B_d\circ T_t|^2 \, ds \\ &+ \int_D \beta_\Omega(x, |\mathbb{M}(t)\nabla\varphi|^2)\mathbb{M}(t)\nabla\varphi\cdot\mathbb{M}(t)\nabla\psi\,\xi(t)\,dx \\ &- \int_D f_0\circ T_t\psi\xi(t)\,dx + \int_{\Omega_{\mathrm{ma}}} M_1\cdot\mathbb{M}(t)\nabla\psi\xi(t)\,dx \\ &+ \int_{D\setminus\overline{\Omega_{\mathrm{ma}}}} M_2\cdot\mathbb{M}(t)\nabla\psi\,\xi(t)\,dx, \end{aligned} \tag{30}$$

where $\mathbb{M}(t) = DT_t^{-T}$ and $\xi(t), \xi_\tau(t)$ are defined in (14) and (15), respectively. Note that we have used the assumption $T_t(\Omega_{\mathrm{ma}}) = \Omega_{\mathrm{ma}}$ in the computation of $\mathfrak{G}(t,\varphi,\psi)$.

Note that $J(\Omega_t) = \mathfrak{G}(t,u^t,\psi)$ for all $\psi\in H_0^1(D)$, where $u^t\in H_0^1(D)$ solves

$$\begin{aligned} &\int_D \beta_\Omega(x, |\mathbb{M}(t)\nabla u^t|^2)\mathbb{M}(t)\nabla u^t\cdot\mathbb{M}(t)\nabla\psi\xi(t)\,dx \\ &\quad = \int_D f_0\circ T_t\psi\xi(t)\,dx - \int_{\Omega_{\mathrm{ma}}} M_1\cdot\mathbb{M}(t)\nabla\psi\xi(t)\,dx - \int_{D\setminus\overline{\Omega_{\mathrm{ma}}}} M_2\cdot\mathbb{M}(t)\nabla\psi\xi(t)\,dx. \end{aligned} \tag{31}$$

To prove Theorem 5, we need to check the conditions of Theorem 3 for the function $\mathfrak{G}(t,\varphi,\psi)$ with $E = F = H_0^1(D)$.

Verification of (H0). Condition (H0)(i) is satisfied since $E(t) = \{u^t\}$, where $u^t\in H_0^1(D)$ is the solution of the state equation (31). Conditions (ii) and (iii) of Assumption (H0) are also satisfied due to the differentiability of the functions β_1,β_2 and Assumption 1. Condition (H0)(iv) is satisfied by construction.

Verification of (H1). Condition (H1) is satisfied since $\mathbb{M}(t)$, $\xi(t)$ and $\xi_\tau(t)$ are smooth.

Verification of (H2). $Y(t,u^t,u^0)=\{p^t\}$, where $p^t\in H_0^1(D)$ is the unique solution of

$$\begin{aligned}\int_0^1\int_D 2\partial_\zeta\beta_\Omega(x,|\mathbb{M}(t)\nabla u_t^s|^2)((\mathbb{M}(t)\nabla u_t^s\otimes\mathbb{M}(t)\nabla u_t^s)\mathbb{M}(t)\nabla p^t)\cdot\mathbb{M}(t)\nabla\psi)\xi(t)\,dx\,ds\\ +\int_0^1\int_D\beta_\Omega(x,|\mathbb{M}(t)\nabla u_t^s|^2)\mathbb{M}(t)\nabla\psi\cdot\mathbb{M}(t)\nabla p^t\xi(t)\,dx\,ds\\ =-\int_0^1\int_{\Gamma_0}2(B_r(u_t^s)-B_d)B_r(\psi)\xi(t)\,dx\,ds\text{ for all }\psi\in H_0^1(D).\end{aligned}\tag{32}$$

which can also be rewritten in a more compact way as

$$\begin{aligned}\int_0^1\int_D\mathcal{A}(\mathbb{M}(t)\nabla u_t^s)\mathbb{M}(t)\nabla p^t\cdot\mathbb{M}(t)\nabla\psi\xi(t)\,dx\,ds\\ =-\int_0^1\int_{\Gamma_0}2(B_r(u_t^s)-B_d)B_r(\psi)\xi(t)\,dx\,ds.\end{aligned}\tag{33}$$

To prove that the previous equation has indeed a unique solution, we first check that all integrals are finite in the previous equation. To verify this, we use Hölder's inequality to obtain

$$\begin{aligned}&\int_D 2\partial_\zeta\beta_\Omega(x,|\mathbb{M}(t)\nabla u_t^s|^2)((\mathbb{M}(t)\nabla u_t^s\otimes\mathbb{M}(t)\nabla u_t^s)\mathbb{M}(t)\nabla p^t)\cdot\mathbb{M}(t)\nabla\psi)\xi(t)\,dx\\ &\le c\left(\int_D 2\partial_\zeta\beta_\Omega(x,|\mathbb{M}(t)\nabla u_t^s|^2)(\mathbb{M}(t)\nabla u_t^s\cdot\mathbb{M}(t)\nabla p^t)^2\,dx\right)^{1/2}\cdot\\ &\qquad\left(\int_D 2\partial_\zeta\beta_\Omega(x,|\mathbb{M}(t)\nabla u_t^s|^2)(\mathbb{M}(t)\nabla u_t^s\cdot\mathbb{M}(t)\nabla\psi)^2\,dx\right)^{1/2}\end{aligned}$$

and

$$\begin{aligned}&\int_D\beta_\Omega(x,|\mathbb{M}(t)\nabla u_t^s|^2)\mathbb{M}(t)\nabla\psi\cdot\mathbb{M}(t)\nabla p^t\xi(t)\,dx\\ &\le c\left(\int_D\beta_\Omega(x,|\mathbb{M}(t)\nabla u_t^s|^2)|\mathbb{M}(t)\nabla\psi|^2\,dx\right)^{1/2}\left(\int_D\beta_\Omega(x,|\mathbb{M}(t)\nabla u_t^s|^2)|\mathbb{M}(t)\nabla p^t|^2\,dx\right)^{1/2}.\end{aligned}$$

Adding both equations and using part 4 of Assumption 1, we get

$$\int_D\mathcal{A}(\mathbb{M}(t)\nabla u_t^s)\mathbb{M}(t)\nabla p^t\cdot\mathbb{M}(t)\nabla\psi\xi(t)\,dx\,ds\le c\|\psi\|_{H^1(D)}\|\bar{p}^t\|_{H^1(D)},\tag{34}$$

where the constant $c>0$ is independent of s.

The existence of a solution p^t follows from Theorem 4. Since $\mathbb{M}(t)=DT_t^{-T}$, there are numbers $C>0$ and $\tau>0$ such that, for all $t\in[0,\tau]$ and $\rho\in\mathbf{R}^2$, we have $\mathbb{M}(t)\rho\cdot\rho\ge C|\rho|^2$. Note that $p^0=p\in Y(0,u^0,u^0)$ is the unique solution of the adjoint equation (23)-(24).

Verification of (H3). To verify this assumption we show that there is a sequence $(p^{t_k})_{k\in\mathbf{N}}$, where $\{p^{t_k}\}=Y(t_k,u^{t_k},u^0)$, which converges weakly in $H_0^1(D)$ to the solution of the adjoint equation and that $(t,\psi)\mapsto\partial_t\mathfrak{G}(t,u^0,\psi)$ is weakly continuous. In order to prove this, we need the following lemmas.

Lemma 3. *Let $m \in \{0,1\}$ and the velocity field $V \in \mathcal{D}^1(\mathbf{R}^2,\mathbf{R}^2)$ be given and $\varphi \in H^m(\mathbf{R}^2)$. We denote by T_t, the transformation associated to V. Then we have*

$$\lim_{t\to 0} \varphi \circ T_t = \varphi \text{ and } \lim_{t\to 0} \varphi \circ T_t^{-1} = \varphi \quad \text{in } H^m(D).$$

Proof. See for instance [7]. □

Recall that according to Remark 2 there are constants $C, \varepsilon > 0$ such that

$$\|u(\chi_1) - u(\chi_2)\|_{H^1(D)} \le \|\chi_1 - \chi_2\|_{L^1(D)}, \quad \forall \chi_1, \chi_2 \in \Xi(D), \tag{35}$$

where

$$\Xi(D) := \{\chi_\Omega : \Omega \subset D \text{ is measurable and } \chi_\Omega(1-\chi_\Omega) = 0 \text{ a.e. in } D\}.$$

With this result it is easy to see that $t \mapsto u^t$ is in fact continuous.

Lemma 4. *Let Assumptions 1.1 to 1.3 hold. Then the mapping $t \mapsto u^t := \Psi_t(u_t)$ is continuous from the right in 0, i.e.,*

$$\lim_{t\searrow 0} \|u^t - u\|_{H_0^1(D)} = 0.$$

If in addition Assumption 1.4 is satisfied, then there are constants $c, \tau > 0$ such that

$$\|u^t - u\|_{H_0^1(D)} \le tc, \quad \text{for all } t \in [0,\tau].$$

Proof. Since $\|\cdot\|_{H_0^1(D)}$ and the L^2-norm of the gradient are equivalent norms on $H_0^1(D)$ it suffices to show $\lim_{t\searrow 0} \|\nabla u^t - \nabla u\|_{L^2(D,\mathbf{R}^d)} = 0$. First of all introduce

$$A_t(x) := \xi(t)(D\Phi_t(x))^{-T}(D\Phi_t(x))^{-1}$$

which satisfies $|A_t(x)^{-1}| \le c$ for all $t \in [0,\tau]$ and hence

$$\begin{aligned} \forall x \in \Omega,\ \forall t \in [0,\tau],\ \forall \zeta \in \mathbf{R}^2 :\ |\zeta|^2 &\le |A_t(x)^{-1}|\, |\xi(t)(D\Phi_t(x))^{-T}\zeta \cdot (D\Phi_t(x))^{-T}\zeta|^2 \\ &= cA_t(x)\zeta\cdot\zeta. \end{aligned} \tag{36}$$

Therefore for all $f_0 \in H^1(D)$ and all $t \in [0,\tau]$

$$\int_D |\nabla(f_0 \circ T_t^{-1})|^2\, dx = \int_D A_t \nabla f_0 \cdot \nabla f_0\, dx \ge \frac{1}{c}\int_D |\nabla f_0|^2\, dx.$$

Further, we get from this estimate that for all $t \in [0,\tau]$

$$c\|f_0\|_{H^1(D)} \le \|f_0 \circ T_t^{-1}\|_{H^1(D)}. \tag{37}$$

Now setting $\chi_1 := \chi_\Omega$ and $\chi_2 := \chi_{\Omega_t} = \chi_\Omega \circ T_t^{-1}$ and denoting the corresponding solutions of (3) by $u := u(\chi_\Omega)$ and $u_t := u(\chi_{\Omega_t})$, we infer from (35) and (37)

$$c\|\nabla(u\circ T_t) - \nabla u^t\|_{L^2(D,\mathbf{R}^d)} \le \|\nabla u_t - \nabla u\|_{L^2(D,\mathbf{R}^d)} \le C\|\chi_\Omega - \chi_\Omega \circ T_t^{-1}\|_{L^1(D)},$$

where $u^t := u_t \circ T_t$. Employing the previous estimates, we get for all $t \in [0,\tau]$

$$\begin{aligned} \|\nabla u - \nabla u^t\|_{L^2(D,\mathbf{R}^d)} &\le \|\nabla u - \nabla(u\circ T_t)\|_{L^2(D,\mathbf{R}^d)} + \|\nabla(u\circ T_t) - \nabla u^t\|_{L^2(D,\mathbf{R}^d)} \\ &\le \tilde{c}\left(\|\nabla u - \nabla(u\circ T_t)\|_{L^2(D,\mathbf{R}^d)} + \|\chi_\Omega - \chi_\Omega \circ T_t^{-1}\|_{L^1(D)}\right). \end{aligned}$$

Finally, taking into account Lemma 3, we obtain the desired continuity. The Lipschitz continuity under the additional Hypothesis 1.4 was shown in [41]. □

Using the previous lemma we are able to show the following.

Lemma 5. *The solution p^t of (32) converges weakly in $H_0^1(D)$ to the solution p of the adjoint equation (23)-(24).*

Proof. The existence of a solution of (32) follows from Theorem 4. Inserting $\psi = p^t$ as test function in (32), we see that the estimate $\|u^t\|_{H^1(D)} \leq C$ implies $\|p^t\|_{H^1(D)} \leq C$ for t sufficient small. From the boundedness, we infer that $(p^t)_{t\geq 0}$ converges weakly to some $w \in H_0^1(D)$. In Lemma 4 we proved $u^t \to u$ in $H_0^1(D)$ which we can use to pass to the limit in (32) and obtain

$$p^{t_k} \rightharpoonup p \text{ in } H_0^1(D) \text{ for } t_k \to 0 \text{ as } k \to \infty,$$

where $p \in H_0^1(D)$ solves the adjoint equation (23)-(24). By uniqueness we conclude $w = p$. □

Now we proceed to the differentiation of (30) at $t > 0$. Introduce the notations $\mathbb{P}(t) = \xi(t)\mathbb{M}(t)$ and $\mathbb{Q}(t) := \xi(t)\mathbb{M}(t)^T\mathbb{M}(t)$, we obtain

$$\begin{aligned}
\partial_t \mathfrak{G}(t,\varphi,\psi) = &\int_{\Gamma_0} \xi_\tau'(t)|B_r(\varphi) - B_d \circ T_t|^2 \, ds \\
&- 2\int_{\Gamma_0} \xi_\tau(t)(B_r(\varphi) - B_d \circ T_t)\nabla B_d \circ T_t \cdot V \, ds \\
&+ 2\int_D \partial_\zeta \beta_\Omega(x, |\mathbb{M}(t)\nabla\varphi|^2)(\mathbb{M}'(t)\nabla\varphi \cdot \mathbb{M}(t)\nabla\varphi)\mathbb{M}(t)\nabla\varphi \cdot \mathbb{M}(t)\nabla\psi\xi(t) \, dx \\
&+ \int_D \beta_\Omega(x, |\mathbb{M}(t)\nabla\varphi|^2)\mathbb{Q}'(t)\nabla\varphi \cdot \nabla\psi \, dx \\
&- \int_D f_0 \circ T_t \, \psi\xi'(t) + \nabla f_0 \circ T_t \cdot V \, \psi\xi(t) \, dx \\
&+ \int_{\Omega_{\mathrm{ma}}} \mathbb{P}'(t)\nabla\psi \cdot M_1 \, dx + \int_{D\setminus\overline{\Omega_{\mathrm{ma}}}} \mathbb{P}'(t)\nabla\psi \cdot M_2 \, dx
\end{aligned} \tag{38}$$

and this shows that for fixed $\varphi \in H_0^1(D)$ the mapping $(t,\psi) \mapsto \partial_t\mathfrak{G}(t,\varphi,\psi)$ is weakly continuous. This finishes proving that (H3) is satisfied.

Consequently, we may apply Theorem 3 and obtain $dJ(\Omega;V) = \partial_t\mathfrak{G}(0,u,p)$, where $u \in H_0^1(D)$ solves the state equation (1)-(2) and $p \in H_0^1(D)$ is a solution of the adjoint equation (23)-(24). In order to compute $\partial_t\mathfrak{G}(0,u,p)$, note that the integrals on Γ_0 vanish due to $V = 0$ on Γ_0, $\mathbb{M}'(0) = -DV^T$, $\mathbb{P}'(0) = (\operatorname{div} V)I_2 - DV^T$, $\mathbb{Q}'(0) = (\operatorname{div} V)I_2 - DV^T - DV$.

Finally we have proved formula (27). This concludes the proof of Theorem 5. ■

6 Optimization of the rotor core

In this section, we use the shape derivative derived in Theorem 5 to determine the optimal design for the electric motor described in Section 2. Recall that the problem consists in finding the shape $\Omega \subset \Omega_f$ of the ferromagnetic subdomain of the electric motor depicted in Fig. 1 which minimizes the cost functional

$$J(\Omega) = \int_{\Gamma_0} |B_r(u_\Omega) - B_d|^2 \mathrm{d}s$$

among all admissible shapes $\Omega \in \mathcal{O}$ where Γ_0 is a circle in the air gap, $B_r(u_\Omega)$ denotes the radial component of the magnetic flux density $B = B(u_\Omega)$ on Γ_0 and B_d is a given sine curve, $B_d(\theta) = \frac{1}{2}\sin(4\,\theta)$ where θ denotes the angle in polar coordinates with origin at the center of the motor; see Fig. 1. Minimizing this functional leads to a reduction of the total harmonic distortion (THD; see [3, 5]) of the flux density which causes the rotor to rotate more smoothly. Here, u_Ω is the solution of the two-dimensional magnetostatic boundary value problem the weak form of which reads as follows:

$$\text{Find } u \in H_0^1(D) \text{ such that } \int_D \nu(|\nabla u|)\nabla u \cdot \nabla v \,\mathrm{d}x = \langle f, v\rangle \text{ for all } v \in H_0^1(D). \tag{39}$$

Here, the right-hand side f corresponds to the weak form of

$$f = f_0 + \operatorname{div} M \text{ with } M = M_1\chi_{\Omega_{\mathrm{ma}}}(x) + M_2\chi_{D\setminus\Omega_{\mathrm{ma}}}(x)$$

as in Section 5, where $f_0 = J_i$, $M_1 = -\frac{\nu}{\nu_0}\binom{-M_y}{M_x}$ and $M_2 = 0$. The vector $\binom{M_x}{M_y}$ denotes the permanent magnetization of the magnets. It is a constant vector in each of the magnet subdomains pointing in the directions indicated in Fig. 1 and vanishes outside the magnet areas. Denoting $M^\perp = \frac{\nu}{\nu_0}\binom{-M_y}{M_x}$, the right hand side $f \in H^{-1}(D)$ reads

$$\langle f, v\rangle = \int_D J_i\, v \;+\; M^\perp \cdot \nabla v \,\mathrm{d}x. \tag{40}$$

The function J_i represents the impressed currents in the coil areas (light blue areas in Fig. 1) and is assumed to vanish in this special application, i.e., $J_i = 0$. We consider admissible shapes $\Omega \in \mathcal{O}$ as in (5) and in Section 5. Furthermore,

$$\nu(|\nabla u|) = \chi_{\Omega_f}\,\hat{\nu}(|\nabla u|) + \chi_{D\setminus\overline{\Omega_f}}\,\nu_0$$

denotes the magnetic reluctivity composed of a nonlinear function $\hat{\nu}$ depending on the magnitude of the magnetic flux density $|B| = |\nabla u|$ inside the ferromagnetic material and a constant $\nu_0 = 10^7/(4\pi)$, which is expressed in the unit $m\,kg\,A^{-2}\,s^{-2}$, otherwise. The constant ν_0 is the magnetic reluctivity of vacuum which is practically the same as that of air. The nonlinear function $\hat{\nu}$ is in practice obtained from measurements and is not available in a closed form. However, the physical properties of magnetic fields yield the following characteristics of $\hat{\nu}$:

(i) $\hat{\nu}$ is continuously differentiable on $(0, \infty)$,

(ii) $\exists\, m > 0 :\ \hat{\nu}(s) \geq m \quad$ for all $s \in \mathbb{R}_0^+$,

(iii) $\hat{\nu}(s) \leq \nu_0 \quad$ for all $s \in \mathbb{R}_0^+$,

(iv) $(\hat{\nu}(s)s)' = \hat{\nu}(s) + \hat{\nu}'(s)s \geq m > 0$,

(v) $s \mapsto \hat{\nu}(s)s$ is strongly monotone with monotonicity constant m, i.e.,

$$(\hat{\nu}(s)\,s - \hat{\nu}(t)\,t)\,(s - t) \geq m(s - t)^2 \quad \text{for all } s, t \geq 0,$$

(vi) $s \mapsto \hat{\nu}(s)s$ is Lipschitz continuous with Lipschitz constant ν_0, i.e.,

$$|\hat{\nu}(s)\,s - \hat{\nu}(t)\,t)| \leq \nu_0|s - t| \text{ for all } \forall s, t \geq 0.$$

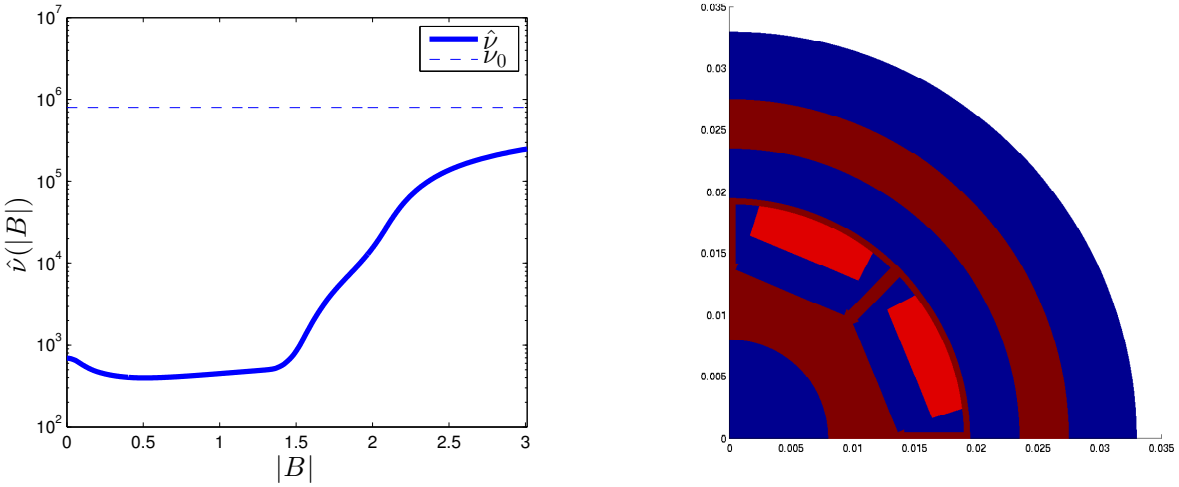

Figure 2: (a) Magnetic reluctivity $\hat{\nu}$ as a function of the magnitude $|B| = |\nabla u|$ of the magnetic flux density. (b) Ferromagnetic material Ω_f with design subdomains $\Omega \subset \Omega_f$ (highlighted).

For more details on properties and practical realization of the function $\hat{\nu}$ from given measurement data, we refer the reader to [16, 24, 35].

In order to be able to apply Theorem 5 to the problem above, we have to check whether Assumption 1 is satisfied for

$$\beta_1(\zeta) := \hat{\nu}(\sqrt{\zeta}) \text{ and } \beta_2(\zeta) := \nu_0.$$

Clearly, all four conditions of Assumption 1 are fulfilled for $\beta_2(\zeta) = \nu_0 = const.$ Now let us investigate more closely β_1. Notice the relations $\beta_1(|\rho|^2) = \hat{\nu}(|\rho|)$ and $\beta_1'(|\rho|^2) = \hat{\nu}'(|\rho|)/(2|\rho|)$.

1. As mentioned above, the function $\hat{\nu}$ is bounded from above by the magnetic reluctivity of vacuum ν_0 and from below by a positive constant m, compare Fig. 2(a).

2. Assumption 1.2 holds for the function $\hat{\nu}$ by virtue of properties (v) and (vi).

3. The numerical realization of the function $\hat{\nu}$ consists in an interproximation of given measurement data. The interproximation was done using splines of class C^1.

4. It is easy to see that this condition for β_1 is equivalent to

$$\exists \lambda,\, \Lambda > 0 : \lambda|\eta|^2 \leq \eta^T \left(\beta_1(|\rho|^2) I_2 + 2\beta_1'(|\rho|^2)\rho \otimes \rho\right) \eta \leq \Lambda|\eta|^2,$$

or in terms of $\hat{\nu}$,

$$\exists \lambda,\, \Lambda > 0 : \lambda|\eta|^2 \leq \eta^T \left(\hat{\nu}(|\rho|) I_2 + \frac{\hat{\nu}'(|\rho|)}{|\rho|}\rho \otimes \rho\right) \eta \leq \Lambda|\eta|^2,$$

where I_2 denotes the identity matrix of dimension 2. The eigenvalues and corresponding eigenvectors of the 2×2 matrix $\hat{\nu}(|\rho|)I_2 + \frac{\hat{\nu}'(|\rho|)}{|\rho|}\rho \otimes \rho$ are given by

$$\lambda_1 = \hat{\nu}(|\rho|) \qquad v_1 = \begin{pmatrix} -\rho_2 \\ \rho_1 \end{pmatrix},$$
$$\lambda_2 = \hat{\nu}(|\rho|) + \hat{\nu}'(|\rho|)|\rho| \qquad v_2 = \begin{pmatrix} \rho_1 \\ \rho_2 \end{pmatrix}.$$

From the physical properties (ii) and (iv) of $\hat{\nu}$ it follows that both λ_1 and λ_2 are positive. Therefore, the assumption holds with $\lambda = \min\{\lambda_1, \lambda_2\}$ and $\Lambda = \max\{\lambda_1, \lambda_2\}$.

Properties (v) and (vi) together with Assumption 1.1 yield existence and uniqueness of a solution $u \in H_0^1(D)$ to the state equation. Assumption 1.4 ensures the existence of an adjoint state $p \in H_0^1(D)$.

Thus we can apply Theorem 5 and the shape derivative is given by (27).

6.1 Numerical method

In each iteration of the optimization process we use the shape derivative $dJ(\Omega; V)$ derived in (27) to compute a vector field V that ensures a decrease of the objective function $dJ(\Omega; V) \leq 0$ by displacing the interface between the iron subdomain Ω and the air subdomain $\Omega^{\text{ref}} \setminus \Omega$ along that vector field.

6.1.1 Setup of interface

Due to practical restrictions we choose not to move the interface by moving the single points of the mesh, as it is common practice in shape optimization. Instead we model the interface by setting up a polygon with 151 points around each of the design subdomains Ω_k^{ref} (see Fig. 3) and move the points of these polygons along the calculated velocity field V in the course of the optimization process. Each element of the design area whose center of gravity is inside this polygon is considered to be ferromagnetic material, the others are considered to be air. That way, we can avoid problems such as deformation of the fixed parts of the motor, i.e. magnets or the air gap, or self-intersections of the mesh.

6.1.2 Descent Direction

In order to get a descent in the cost functional, we compute the velocity field as follows. We choose a symmetric and positive definite bilinear form

$$b : H_0^1(D_{\text{rot}}) \times H_0^1(D_{\text{rot}}) \to \mathbb{R}$$

defined on the subdomain D_{rot} of D representing the rotor and compute V as the solution of the variational problem:

$$\text{Find } V \in P_h \text{ such that } b(V, W) = -dJ(\Omega, W) \text{ for all } W \in P_h, \tag{41}$$

where $P_h \subset H_0^1(D_{\text{rot}})$ is a finite dimensional subspace. Outside D_{rot} we extend V by zero. Note that, by this choice, the condition $V = 0$ on Γ_0, which is assumed in Section 5, is satisfied. The obtained descent directions $V \in P_h$ will also be in $W^{1,\infty}(D, \mathbf{R}^2)$

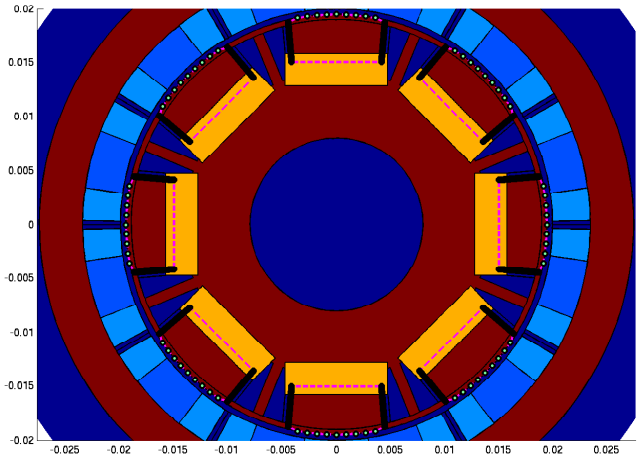

(a)

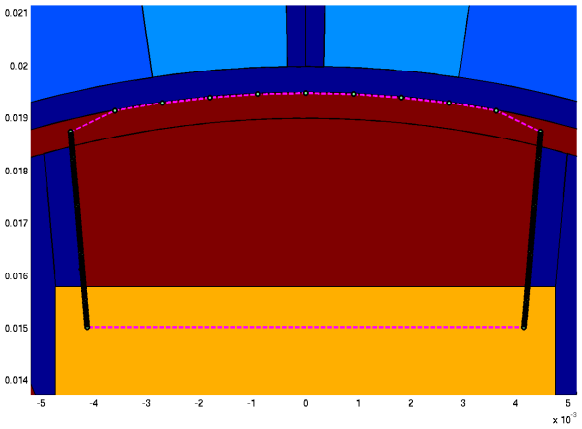

(b)

Figure 3: (a) Interface points around eight design areas of the electric motor. (b) Zoom on the upper design area: Fictitious interface polygon consists of 151 points (71 on the left, 71 on the right and 9 on top)

and, consequently, they are admissible vector fields defining a flow T_t^V. The solution V computed this way is a descent direction for the cost functional since

$$dJ(\Omega, V) = -b(V, V) \leq 0.$$

For our numerical experiments, we choose the bilinear form

$$\begin{aligned} b : H_0^1(D_{\text{rot}}) \times H_0^1(D_{\text{rot}}) &\to \mathbb{R} \\ b(V, W) &= \int_{D_{\text{rot}}} (\alpha \, \mathrm{D}V : \mathrm{D}W + V \cdot W) \, \mathrm{d}x. \end{aligned} \tag{42}$$

Here, the penalization function $\alpha \in L^\infty(D_{\text{rot}})$ is chosen as

$$\alpha(x) = \begin{cases} 1 & x \in \Omega \\ 10 & x \in \Omega^\varepsilon \setminus \Omega \\ 10^2 & \text{else,} \end{cases}$$

where $\Omega^\varepsilon = \{x \in D_{\text{rot}} : \operatorname{dist}(x, \Omega) \leq \varepsilon\}$ for some small $\varepsilon > 0$. With this choice of α, we ensure that the resulting velocity field V is small outside the design region Ω^{ref}.

For all numerical simulations, we used piecewise linear finite elements on a triangular grid with 44810 degrees of freedom and 89454 elements where we chose a particularly fine discretization in the design regions Ω^{ref} (53488 design elements). The nonlinear state equation (1) is solved by Newton's method. All arising linear systems of finite element equations are solved using the parallel direct solver PARDISO [12].

6.1.3 Updating the interface

For updating the interface, we perform a backtracking (line search) algorithm: Once a descent direction V is computed, we move all interface points a step size $\tau = \tau_{init}$ in the

direction given by V and evaluate the cost function for the updated geometry. If the cost value has not decreased, the step size τ is halved and the cost function is evaluated for the new, updated geometry. We repeat this step until a decrease of the cost function has been achieved. When the step size becomes too small such that no element switches its state, the algorithm is stopped.

6.2 Numerical Results

The procedure is summarized in Algorithm 1:

Algorithm 1. *Set converged = false*
While !converged

1. *Compute state u using* (1) *and adjoint state p using* (22).
2. *Compute shape derivative $dJ(\Omega; V)$ from* (27).
3. *Compute descent direction V using* (41).
4. *Find step width τ that yields a decrease in the cost function using backtracking.*
5. *If decrease in the cost function could be achieved:*

   Update interface and go to step 1.

   else:

   converged = true.

The final design after 35 iterations of Algorithm 1 can be seen in Fig. 4. The cost function is reduced from $1.3033 * 10^{-3}$ to $0.94997 * 10^{-3}$, i.e., by about 27%. The radial component of the magnetic field on the circle Γ_0 in the air gap for the initial (blue), desired (green) and final design (red) can be seen in Fig. 5. The optimization process took about 26 minutes using a single core on a laptop.

7 Conclusion

In this paper, we have performed the rigorous analysis of the shape sensitivity analysis of a subregion Ω of the rotor of an electric motor in order to match a certain rotation pattern. The shape derivative of the cost functional was computed efficiently using a shape-Lagrangian method for nonlinear partial differential equation constraints which allows to bypass the computation of the material derivative of the state. The implementation of the obtained shape derivative in a numerical algorithm provides an interesting shape which allows us to improve the rotation pattern. In the numerical experiment presented in this work, we chose a rather simple way of updating the interface: We just switched the state of single elements of the finite element mesh as discrete entities. For a more accurate resolution of the interface, one may employ a nonstandard finite element method like the extended Finite Element Method (XFEM) [33] or the immersed FEM [30], or a discontinuous Galerkin approach based on Nitsche's idea, see [13]. These approaches make it possible to represent an interface that is not aligned with the underlying

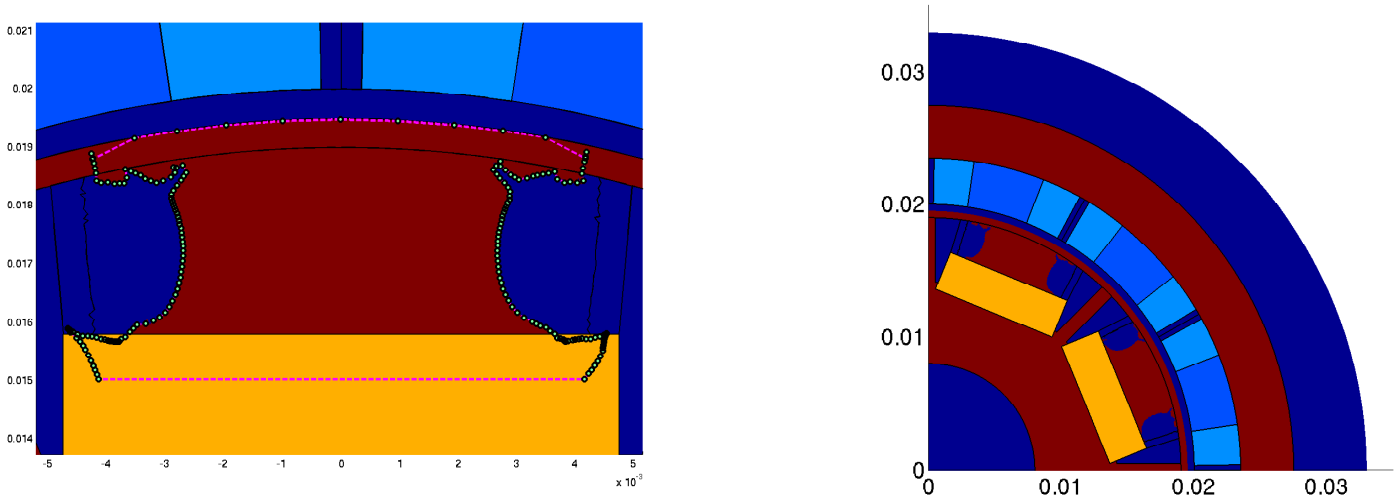

(a) (b)

Figure 4: (a) Final design of one component Ω_k after 35 iterations of Algorithm 1. (b) Upper-right quarter of the optimized motor.

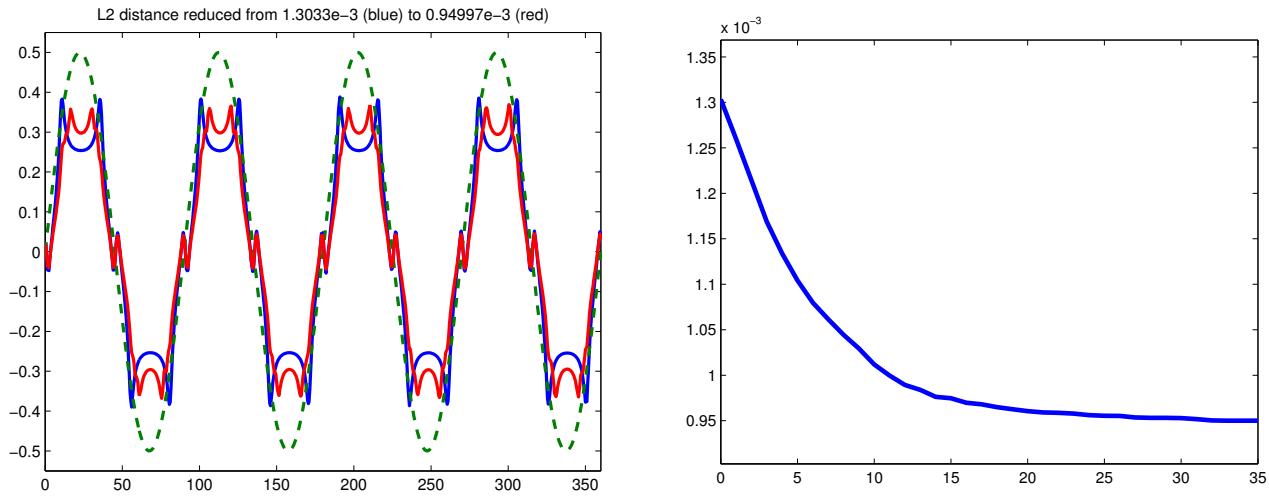

(a) (b)

Figure 5: (a) Radial component of the magnetic flux density B along curve Γ_0 in air gap: initial design (blue), desired sine curve B_d (green), final design (red). (b) Decrease of cost functional in the course of the optimization process.

FE discretization without loss of accuracy. An alternative way to achieve this would be to locally modify the finite element basis in a parametric way as it is done in [8].

Acknowledgments. Antoine Laurain and Houcine Meftahi acknowledge financial support by the DFG Research Center Matheon "Mathematics for key technologies" through the MATHEON-Project C37 "Shape/Topology optimization methods for inverse problems". Peter Gangl and Ulrich Langer gratefully acknowledge the Austrian Science Fund (FWF) for the financial support of their work via the Doctoral Program DK W1214 (project DK4) on Computational Mathematics. They also thank the Linz Center of Mechatronics (LCM), which is a part of the COMET K2 program of the Austrian Government, for supporting their work on topology and shape optimization of electrical machines.

References

[1] S. Amstutz and A. Laurain. A semismooth Newton method for a class of semilinear optimal control problems with box and volume constraints. *Computational Optimization and Applications*, 56(2):369–403, 2013.

[2] R. Arumugam, J. Lindsay, D. Lowther, and R. Krishnan. Magnetic field analysis of a switched reluctance motor using a two dimensional finite element model. *IEEE Trans. Magn.*, 21(5):1883–1885, 1985.

[3] A. Binder. *Elektrische Maschinen und Antriebe: Grundlagen, Betriebsverhalten*. Springer-Lehrbuch. Springer, 2012.

[4] A. Bonnafé. *Développements asymptotiques topologiques pour une classe d'équations elliptiques quasi-linéaires. Estimations et développements asymptotiques de p-capacités de condensateur. Le cas anisotrope du segment*. PhD thesis, Université de Toulouse, France, 2013.

[5] J. Choi, K. Izui, S. Nishiwaki, A. Kawamoto, and T. Nomura. Rotor pole design of IPM motors for a sinusoidal air-gap flux density distribution. *Structural and Multidisciplinary Optimization*, 46(3):445–455, 2012.

[6] J. S. Choi, K. Izui, A. Kawamoto, S. Nishiwaki, and T. Nomura. Topology optimization of the stator for minimizing cogging torque of IPM motors. *IEEE Trans. Magn.*, 47(10):3024–3027, 2011.

[7] M. C. Delfour and J.-P. Zolésio. *Shapes and geometries*, volume 22 of *Advances in Design and Control*. Society for Industrial and Applied Mathematics (SIAM), Philadelphia, PA, second edition, 2011. Metrics, analysis, differential calculus, and optimization.

[8] S. Frei and T. Richter. A locally modified parametric finite element method for interface problems. *SIAM J. Numer. Anal.*, 52(5):2315–2334, 2014.

[9] G. Frémiot, W. Horn, A. Laurain, M. Rao, and J. Sokołowski. On the analysis of boundary value problems in nonsmooth domains. *Dissertationes Math. (Rozprawy Mat.)*, 462:149, 2009.

[10] P. Fulmański, A. Laurain, J.-F. Scheid, and J. Sokołowski. A level set method in shape and topology optimization for variational inequalities. *Int. J. Appl. Math. Comput. Sci.*, 17(3):413–430, 2007.

[11] P. Gangl and U. Langer. Topology optimization of electric machines based on topological sensitivity analysis. *Computing and Visualization in Science*, 2014.

[12] K. Gartner and O. Schenk. Solving unsymmetric sparse systems of linear equations with PARDISO. *J. of Future Generation Computer Systems*, 20(3):475–487, 2004.

[13] A. Hansbo and P. Hansbo. An unfitted finite element method, based on Nitsche's method, for elliptic interface problems. *Computer Methods in Applied Mechanics and Engineering*, 191(47-48):5537 – 5552, 2002.

[14] J. Haslinger and R. Mäkinen. *Introduction to Shape Optimization*. Society for Industrial and Applied Mathematics, 2003.

[15] J. Haslinger and P. Neittaanmäki. *Finite Element Approximation for Optimal Shape, Material and Topology Design*. Wiley, 1996.

[16] B. Heise. Analysis of a fully discrete finite element method for a nonlinear magnetic field problem. *SIAM J. Numer. Anal.*, 31(3):745–759, 1994.

[17] A. Henrot and M. Pierre. *Variation et optimisation de formes*, volume 48 of *Mathématiques & Applications (Berlin) [Mathematics & Applications]*. Springer, Berlin, 2005. Une analyse géométrique. [A geometric analysis].

[18] M. Hintermüller and A. Laurain. A shape and topology optimization technique for solving a class of linear complementarity problems in function space. *Comput. Optim. Appl.*, 46(3):535–569, 2010.

[19] M. Hintermüller and A. Laurain. Optimal shape design subject to elliptic variational inequalities. *SIAM J. Control Optim.*, 49(3):1015–1047, 2011.

[20] J.-P. Hong, J. Kwack, and S. Min. Optimal stator design of interior permanent magnet motor to reduce torque ripple using the level set method. *IEEE Trans. Magn.*, 46(6):2108–2111, 2010.

[21] M. Iguernane, S. A. Nazarov, J.-R. Roche, J. Sokolowski, and K. Szulc. Topological derivatives for semilinear elliptic equations. *Int. J. Appl. Math. Comput. Sci.*, 19(2):191–205, 2009.

[22] K. Ito, K. Kunisch, and Z. Li. Level-set function approach to an inverse interface problem. *Inverse Problems*, 17(5):1225–1242, 2001.

[23] M. Jung and U. Langer. *Methode der finiten Elemente für Ingenieure: Eine Einführung in die numerischen Grundlagen und Computersimulation*. Springer-Vieweg–Verlag, Darmstadt, 2013. 2., überarb. u. erw. Aufl., 639 S.

[24] B. Jüttler and C. Pechstein. Monotonicity-preserving interproximation of B-H-curves. *J. Comp. App. Math.*, 196:45–57, 2006.

[25] J. Kolota and S. Steien. Analysis of 2D and 3D finite element approach of a switched reluctance motor. *Przeglad Elektrotechniczny (Electrical Review),*, 87(12a):188–190, 2011.

[26] E. Laporte and P. L. Tallec. *Numerical Methods in Sensitivity Analysis and Shape Optimization.* Modeling and Simulation in Science, Engineering & Technology. Birkhäuser, 2003.

[27] A. Laurain. Global minimizer of the ground state for two phase conductors in low contrast regime. *ESAIM: Control, Optimisation and Calculus of Variations*, 20:362–388, 4 2014.

[28] A. Laurain, M. Hintermüller, M. Freiberger, and H. Scharfetter. Topological sensitivity analysis in fluorescence optical tomography. *Inverse Problems*, 29(2):025003, 30, 2013.

[29] A. Laurain and K. Sturm. Domain expression of the shape derivative and application to electrical impedance tomography. Technical Report 1863, Weierstrass Institute for Applied Analysis and Stochastics, 2013.

[30] Z. Li, T. Lin, and X. Wu. New cartesian grid methods for interface problems using the finite element formulation. *Numer. Math.*, 96:61–98, 2003.

[31] D. Miyagi, S. Shimose, N. Takahashi, and T. Yamada. Optimization of rotor of actual IPM motor using ON/OFF method. *IEEE Trans. Magn.*, 47(5):1262–1265, 2011.

[32] D. Miyagi, N. Takahashi, and T. Yamada. Examination of optimal design on IPM motor using ON/OFF method. *IEEE Trans. Magn.*, 46(8):3149–3152, 2010.

[33] N. Mos, J. Dolbow, and T. Belytschko. A finite element method for crack growth without remeshing. *Int. J. Numer. Meth. Engng.*, 46(1):131–150, 1999.

[34] A. A. Novotny and J. Sokołowski. *Topological derivatives in shape optimization.* Interaction of Mechanics and Mathematics. Springer, Heidelberg, 2013.

[35] C. Pechstein. Multigrid-Newton-methods for nonlinear magnetostatic problems. Master's thesis, Johannes Kepler University Linz, 2004.

[36] C. Pechstein. *Finite and Boundary Element Tearing and Interconnecting Methods for Multiscale Elliptic Partial Differential Equations.* PhD thesis, Johannes Kepler University Linz, 2008.

[37] O. Pironneau. *Optimal shape design for elliptic systems.* Springer Series in Computational Physics. Springer-Verlag, New York, 1984.

[38] S. Schmidt, C. Ilic, V. Schulz, and N. Gauger. Three-dimensional large-scale aerodynamic shape optimization based on shape calculus. *AIAA Journal*, 51(11), November 2013.

[39] J. Sokołowski and A. Żochowski. On the topological derivative in shape optimization. *SIAM J. Control Optim.*, 37(4):1251–1272, 1999.

[40] J. Sokołowski and J.-P. Zolésio. *Introduction to shape optimization*, volume 16 of *Springer Series in Computational Mathematics*. Springer-Verlag, Berlin, 1992. Shape sensitivity analysis.

[41] K. Sturm. Lagrange method in shape optimization for non-linear partial differential equations: A material derivative free approach. Technical Report 1817, Weierstrass Institute for Applied Analysis and Stochastics, 2013.

[42] H. Torkaman and E. Afjei. Comprehensive study of 2-D and 3-D finite element analysis of a switched reluctance motor. *J. Appl. Sciences*, 8(15):2758–2763, 2008.

[43] G. Weidenholzer, S. Silber, G. Jungmayr, G. Bramerdorfer, H. Grabner, and W. Amrhein. A flux-based PMSM motor model using RBF interpolation for time-stepping simulations. In *Electric Machines Drives Conference (IEMDC), 2013 IEEE International*, pages 1418–1423, May 2013.

[44] E. Zeidler. *Applied Functional Analysis: Applications to Mathematical Physics*, volume 108 of *Appl. Math. Sci.* Springer New York, 1995.

Latest Reports in this series

2009 - 2012

[..]

2013

[..]

2013-06	Peter Gangl and Ulrich Langer *Topology Optimization of Electric Machines Based on Topological Sensitivity Analysis*	September 2013
2013-07	Walter Zulehner *The Ciarlet-Raviart Method for Biharmonic Problems on General Polygonal Domains: Mapping Properties and Preconditioning*	October 2013
2013-08	Wolfgang Krendl, Valeria Simoncini and Walter Zulehner *Efficient Preconditioning for an Optimal Control Problem with the Time-periodic Stokes Equations*	November 2013

2014

2014-01	Helmut Gfrerer and Jiří V. Outrata *On Computation of Generalized Derivatives of the Normal-Cone Mapping and their Applications*	May 2014
2014-02	Helmut Gfrerer and Diethard Klatte *Quantitative Stability of Optimization Problems and Generalized Equations*	May 2014
2014-03	Clemens Hofreither and Walter Zulehner *On Full Multigrid Schemes for Isogeometric Analysis*	May 2014
2014-04	Ulrich Langer, Sergey Repin and Monika Wolfmayr *Functional A Posteriori Error Estimates for Parabolic Time-Periodic Boundary Value Problems*	July 2014
2014-05	Irina Georgieva and Clemens Hofreither *Interpolating Solutions of the Poisson Equation in the Disk Based on Radon Projections*	July 2014
2014-06	Wolfgang Krendl and Walter Zulehner *A Decomposition Result for Biharmonic Problems and the Hellan-Herrmann-Johnson Method*	July 2014
2014-07	Martin Jakob Gander and Martin Neumüller *Analysis of a Time Multigrid Algorithm for DG-Discretizations in Time*	September 2014
2014-08	Martin Jakob Gander and Martin Neumüller *Analysis of a New Space-Time Parallel Multigrid Algorithm for Parabolic Problems*	November 2014
2014-09	Helmut Gfrerer and Jiří V. Outrata *On Computation of Limiting Coderivatives of the Normal-Cone Mapping to Inequality Systems and their Applications*	December 2014

2015

2015-01	Peter Gangl, Ulrich Langer, Antoine Laurain, Houcine Meftahi and Kevin Sturm *Shape Optimization of an Electric Motor Subject to Nonlinear Magnetostatics*	January 2015

From 1998 to 2008 reports were published by SFB013. Please see
`http://www.sfb013.uni-linz.ac.at/index.php?id=reports`
From 2004 on reports were also published by RICAM. Please see
`http://www.ricam.oeaw.ac.at/publications/list/`
For a complete list of NuMa reports see
`http://www.numa.uni-linz.ac.at/Publications/List/`